A Comparison of Various Kinematic Models for Sandwich Shell Panels with Soft Core

E. CARRERA AND S. BRISCHETTO*
Department of Aeronautics and Space Engineering, Politecnico di Torino, Italy

ABSTRACT: A large variety of classical and advanced shell theories are assessed in the present work to evaluate bending response of sandwich shell structures with soft core. The accuracy of classical, higher order, zig-zag, layer-wise, and mixed theories is compared in the case of closed form solutions of simply supported shell panels made by two external skins and an internal soft core. Thickness strain effects have been evaluated too. The various theories have been implemented in a compact and concise form by referring to Carrera's unified formulation (CUF) for plate/shell analysis that has been, in the recent past, introduced by the first author. Shell theories accuracy has been established with respect to a geometrical parameter (length-to-thickness-ratio) and to a mechanical one (face-to-core-stiffness-ratio). Soft core cases have been mostly analyzed. Two main sources of error have been outlined, which are related to the geometrical parameter and to the mechanical one, respectively. It has been concluded that higher order theories (HOTs) can be conveniently used to reduce the error due to the geometrical parameter in thick shell cases. HOTs are instead not effective to increase the accuracy of classical theories analysis whenever the error is caused by increasing values of the mechanical parameter; layer-wise analysis becomes mandatory in this last case. Among the considered equivalent single layer theories, of particular interest are those zig-zag theories that make use of Murakami's zig-zag function.

KEY WORDS: sandwich shells, soft core, classical 2D theories, equivalent single layer theories, layer wise theories, Murakami's zig-zag function, mixed models, Carrera's unified formulation.

INTRODUCTION

IN THE AIRCRAFT, spacecraft ships and automotive vehicles, sandwich structures are used to provide a stronger and stiffer structure for the same weight, or conversely a lighter structure to carry the same load as a homogenous or compact-laminate flexural member. Usually, these structures are constituted by two stiff skins (faces) and a soft core, this last in recent applications is made by metallic foams.

*Author to whom correspondence should be addressed. E-mail: salvatore.brischetto@polito.it
Figures 2–7 appear in color online: http://jcm.sagepub.com

0021-9983/09/20 2201–21 $10.00/0 DOI: 10.1177/0021998309343716

The books by Plantema [1], Allen [2], Zenkert [3], and Vinson [4] discuss the main aspects considered in the design, analysis, and construction of sandwich structures. Among these issues, our interest is in the work directed to compare shell theories able to provide accurate evaluations of stress/strain fields in each layer in order to prevent failure mechanisms. 3D elasticity solutions, see [5–7], could be used to this purpose. But, the use of 2D plate/shell models is preferred in most of the applications related to sandwich structures. 2D models are, in fact, more convenient than 3D ones in terms of required computational efforts. Various 2D models have been developed in the literature. A large variety of refined theories have been directed to improve the response of classical models which are based on the well known hypothesis by Cauchy–Poisson–Kirchhoff–Love [8–11] and by Reissner–Mindlin [12,13].

Refined theories became more attractive with the advent of composite materials in aerospace structures, because of these materials are, as definition, multilayered made. The main novelties involving composite materials are: – composite materials show high transverse shear and normal deformability with respect to metallic ones, – zig-zag (ZZ) form of the displacement field in the thickness direction (the displacement field shows discontinuous slope at each layer interface), – the interlaminar continuity (IC) of transverse shear and normal stresses should be considered by refined models. ZZ and IC were referred to as C_z^0–Requirements in [14], that is displacement and transverse stress variables are C^0-continuous functions (piece-wise) in the z-thickness direction while their derivatives could be discontinuous at interface. The textbooks by Lekhnitskii [15], Ambartsumian [16-18], Librescu [19], and Reddy [20] on multilayered structures modeling could provide a review on available approaches vs. refined models for layered structures. Many survey articles have been published on sandwich and multilayered structures modelings, some of these are reported in a review article by the first author [21] and a survey companion paper [22]. Of particular interest are the works by Zhong and Reimerders [23] that use a higher–order theory based on a three-layer model and Demiray et al. [24] that introduce a triangular high-order finite element for sandwich plates with transversely compressible core. Frostig [25] proposes a closed form approach based on variational principles. The effects of the transversely flexible core are incorporated resulting in nonlinear patterns. An other higher-order sandwich shell theory is an effective multilayer formulation proposed by Hohe et al. [26]. Hohe and Librescu [27] consider an advanced geometrically nonlinear shell theory for doubly curved structural sandwich panels with transversely compressible core. The model is based on the Kirchhoff theory for the face sheets and a second/third order power expansion for the core. Over 800 references on sandwich structures are considered in Noor et al. [28] and in Reddy and Robbins [29].

A first classification of the 2D models for layered/sandwich structures could be made considering the variable description in the layers. Layer-wise models (LWMs) are those in which the number of the variables is independent in each layer. ZZ effects is intrinsically considered in the LWMs. IC cannot be *a priori* guaranteed by LWMs. Equivalent single layer models (ESLMs) preserve the number of the unknown variables independent by the number of the constitutive layers. Secondly, 2D theories can be distinguished by the choice of the primary variables. If only displacements are used, the corresponding model can be referred as *classical* and the related models could be formulated on the basis of Principle of virtual displacements (PVD). If stresses are also employed as unknowns the related models are refereed to as *mixed* ones. Among the various mixed variational statements the Reissner's mixed variational theorem (RMVT), which was proposed in [30] and

over-viewed in [31], appears very suitable for multilayered structures since only transverse stresses are added to displacements in order to fulfill IC.

In most of the available papers on sandwich structures modeling, it happens that a proposed refined theory is only compared to available 3D solution and/or to CLT/FSDT classical results. In very few cases the comparison is extended to refined theories. This is, of course, an understandable limitation: it appears obvious that HOTs will improve CLT/FSDT results and will not be better than 3D analysis, hence this limitation does not offer the possibility to establish the effective capability of a given HOT with respect to available others. It is concluded that a complete numerical assessment of the most used refined and advanced theories for the static and dynamic analysis of sandwich structures is not available in both cases of plate and shell structures. The plate geometry had just been investigated in [22], the second one will be expanded in this new companion paper.

In the last years Carrera and co-authors [14], [32–36] have proposed a unified formulation (UF) of multilayered theories in the framework of both PVD and RMVT applications. Classical models formulated on the basis of PVD and mixed models based on RMVT were both considered. LW and ESL models related to linear to fourth order expansion in the plate/shell thickness direction z were implemented. ZZ, IC, transverse shear, and normal strains effects were addressed. Navier-type closed form solutions were obtained.

This article reconsiders the findings in the companion paper [22] for plates, to provide a comprehensive numerical assessment of sandwich shell theories for the evaluation of static response of curved panels. The following two parameters have been used in the analysis: a geometrical parameter, called Length-to-thickness-ratio (LTR) that in case of shells is represented by the ratio between the no-zero radius of curvature and the thickness (R/h); a mechanical one, called Face-to-core-stiffness-ratio (FCSR). By varying LTR and FCSR the various sandwich theories are compared in terms of displacements and stresses. Mostly, the following theories are considered: classical theories (CLT, FSDT); HOTs up-to forth-order of expansion in the thickness direction; HOTs including Murakami's ZZ functions; layer-wise analysis up-to forth order of expansion in each layer; mixed ESLMs and LW theories based on the Reissner's mixed variational theorem. Errors with respect to 3D solutions are provided to establish the accuracy of a given analysis.

Classical, higher order, layers-wise and mixed theories are shortly described in sections 'Classical Theories, CLT and FSDT', 'High Order Theories, HOTs', 'Layer-wise Theories, LWTs', and 'Mixed Theories Based on Reissness Mixed Variational Theorem'. Results and discussions are provided in section 'Results and Discussion'.

CLASSICAL THEORIES, CLT AND FSDT

In order to explore how the various kinematic assumptions can affect the response of sandwich shells, a large variety of plates/shells theories have been considered in the present work. A short discussion is given in the following, as just done for the plate case in [22].

Shells of constant thickness h and constant radii of curvature R_α and R_β are considered. The geometry and reference system are shown in Figure 1. α, β, and z is the reference system along whose directions the three displacement components u_α, u_β, and u_z are measured. z denotes the thickness direction and Ω is the shell reference surface.

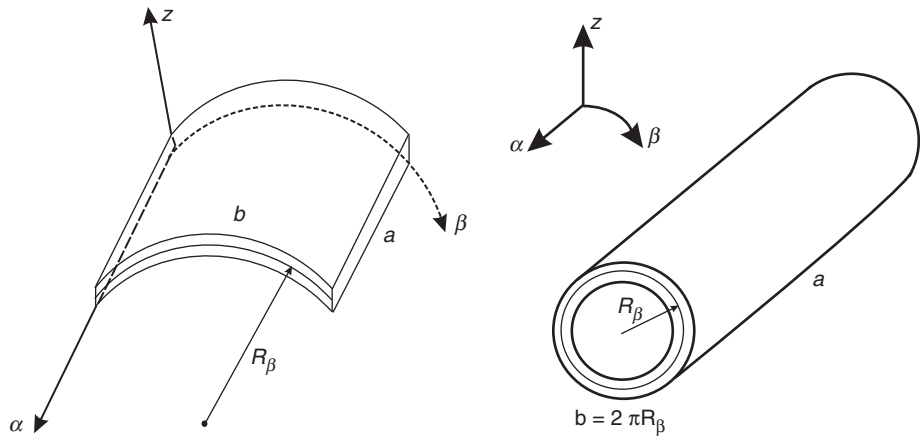

Figure 1. *Geometry and notations for the Ren (left) and Varadan and Baskar (right) shells.*

Plain-stress/plain-strain conditions for the whole considered theories have been imposed according to the recent analyses reported in [35,36].

Classical Lamination Theory

Classical Lamination Theory (CLT), based on Cauchy [8], Poisson [9], or Kirchhoff [10] type assumptions, discards transverse shear and trough-the-thickness deformations. The displacement model related to CLT can be written in the following form:

$$u_\tau(\alpha, \beta, z) = u_{0\tau}(\alpha, \beta) - z \frac{\partial u_{0z}(\alpha, \beta)}{\partial \tau}, \qquad \tau = \alpha, \beta, \tag{1}$$

$$u_z(\alpha, \beta, z) = u_{0z}(\alpha, \beta), \tag{2}$$

which states that the section remain plane and orthogonal to the shell reference surface Ω. u_0 denotes the displacements value in correspondence to the reference surface Ω.

Transverse shear stresses are discarded by CLT analysis. Plane-stress conditions are imposed as in [35,36].

First-order Shear Deformation Theory

Transverse shear deformation can be introduced in above theory according to the following kinematic assumptions, known as Reissner–Mindlin [12,13] ones:

$$u_\tau(\alpha, \beta, z) = u_{0\tau}(\alpha, \beta) + z u_{1\tau}(\alpha, \beta), \qquad \tau = \alpha, \beta, \tag{3}$$

$$u_z(\alpha, \beta, z) = u_{0z}(\alpha, \beta), \tag{4}$$

this theory is also denoted as first-order shear deformation theory (FSDT).

Transverse shear stresses show '*a priori*' constant piece-wise distribution. As in the CLT case, plane-stress conditions are imposed as just shown in [35,36].

HIGHER ORDER THEORIES

HOTs Including and Neglecting Transverse Normal Strains

Higher order terms can be introduced in the kinematic assumptions made for the displacements field in order to obtain refinements of CLT and FSDT analyses:

$$u_\tau(\alpha, \beta, z) = u_{0\tau}(\alpha, \beta) + z^i u_{i\tau}(\alpha, \beta), \qquad \tau = \alpha, \beta, z, \qquad i = 1, N. \tag{5}$$

The summing convention for the repeated indexes has been adopted; N is the order of expansion, which is taken as a free parameter. In this article, the values $N=1$ up to $N=4$ are considered in the numerical investigation. According to Carrera's Unified Formulation (CUF), the related theories will be denoted as $ED1 - ED4$. The letter E denotes that the kinematic is preserved for the whole layers of the shell, as in the so-called equivalent single layer (ESL) approach. D denotes that only displacement unknowns are used and the last number denotes the order of the expansion in z.

The following condition should be considered for the transverse displacement in case transverse normal strains are discarded:

$$u_z(\alpha, \beta, z) = u_{0z}(\alpha, \beta). \tag{6}$$

Related theories are denoted by adding the suffix d to acronyms $ED1 - ED4$: $ED1d - ED4d$.

HOTs Including ZZ Effects

The EDN models are not able to describe ZZ effects [21] in case of laminates. The discontinuity of the first derivative with correspondence to the layer interfaces, can be introduced by employing Murakami's ZZ function (MZZF) [37], that was proposed in the framework of RMVT applications in [38]. The not dimensioned layer coordinate $\zeta_k = (2z_k)/h_k$ is further introduced (h_k is the thickness of the kth layer, z_k is the layer thickness coordinate). MZZF $M(z)$ was defined according to the following formula:

$$M(z) = (-1)^k \zeta_k. \tag{7}$$

$M(z)$ has the following properties: it is piece-wise linear function of the layer coordinate z_k; $M(z)$ has unit amplitude for the whole layers; the slope $M'(z) = \frac{dM}{dz}$ assumes opposite sign between two-adjacent layers (its amplitude is layer thickness dependent). The displacement including MZZF is written in the form:

$$u_\tau(\alpha, \beta, z) = u(\alpha, \beta)_{0\tau} + z^r u(\alpha, \beta)_{r\tau} + (-1)^k \zeta_k u(\alpha, \beta)_{Z\tau}, \quad \tau = \alpha, \beta, z, \quad r = 1, 2, \ldots, N. \tag{8}$$

Subscripts $_Z$ refers to the introduced ZZ term. Higher order distributions in the z-direction are introduced by the r-polynomials.

Modifications of EDN directed to include MZZF are herein denoted as EDZN analysis. It is anticipated that the use of MZZF will result very beneficial in the modeling of sandwich structures.

LAYER-WISE THEORIES

Multilayered shells can be analyzed by kinematic assumptions which are independent in each layer. According to [20] these approaches have herein stated as LWTs.

Layer-wise description requires assuming independent displacement variables in each k-layer. The Taylor thickness expansion used for ESL cases of the previous paragraphs, is not convenient for layer-wise description. Interlaminar continuity for displacements can be more conveniently imposed by employing interface values as unknown variables. Therefore, layer-wise description is written according to the following expansion:

$$u_\tau^k = F_t \; u_{\tau t}^k \; + \; F_b \, u_{\tau b}^k \; + \; F_r \; u_{\tau r}^k, \quad \tau = \alpha, \beta, z, \quad r = 2, 3, \ldots, N, \quad k = 1, 2, \ldots, N_l. \tag{9}$$

It is intended that the subscripts t and b denote values related to the layer top and bottom surface, respectively. N_l is the number of layers. The thickness functions $F_\tau(\zeta_k)$ have been defined by

$$F_t = \frac{P_0 + P_1}{2}, \quad F_b = \frac{P_0 - P_1}{2}, \quad F_r = P_r - P_{r-2}, \qquad r = 2, 3, \ldots, N, \tag{10}$$

in which $P_j = P_j(\zeta_k)$ is the Legendre polynomial of the jth order defined in the ζ_k–domain : $-1 \leq \zeta_k \leq 1$. Fourth order case will be used in the numerical investigations; related polynomials are:

$$P_0 = 1\,, \quad P_1 = \zeta_k, \quad P_2 = (3\zeta_k^2 - 1)/2, \quad P_3 = \frac{5\zeta_k^3}{2} - \frac{3\zeta_k}{2}, \quad P_4 = \frac{35\zeta_k^4}{8} - \frac{15\zeta_k^2}{4} + \frac{3}{8}.$$

The chosen functions have the following interesting properties:

$$\zeta_k = \begin{cases} 1 & : \quad F_t = 1; \quad F_b = 0; \quad F_r = 0 \\ -1 & : \quad F_t = 0; \quad F_b = 1; \quad F_r = 0. \end{cases} \tag{11}$$

The top and bottom values have been used as unknown variables. The interlaminar compatibility of displacement can be therefore easily linked:

$$u_{\tau t}^k = u_{\tau b}^{(k+1)}, \quad k = 1, \; N_l - 1. \tag{12}$$

The used acronyms for these theories are $LD1 - LD4$, where L means Layer-Wise approach.

MIXED THEORIES BASED ON REISSNER'S MIXED VARIATIONAL THEOREM

It is well known fact [31], that the kinematic above described, if applied to multilayered structures, is not able to furnish interlaminar continuous of transverse shear and normal stresses at the interfaces between two adjacent layers. Reissner's Mixed Variational Theorem [30,31] offers a possibility to fulfill '*a priori*' the interlaminar continuity. Both displacements and transverse shear/normal stresses can be assumed in the RMVT framework as primary variables.

Layerwise Mixed Theories

In the layer wise case the displacement model at Equation (9) is also used for the transverse shear/normal stresses:

$$\sigma^k_{\tau z} = F_t\, \sigma^k_{\tau z_t} + F_b\, \sigma^k_{\tau z_b} + F_r\, \sigma^k_{\tau z_r}, \quad \tau = \alpha, \beta, z,\ r = 2, 3, \ldots, N,\ k = 1, 2, \ldots, N_l. \quad (13)$$

The interlaminar transverse shear and normal stresses continuity can be therefore easily linked:

$$\sigma^k_{\tau z_t} = \sigma^{(k+1)}_{\tau z_b}, \quad \tau = \alpha, \beta, z, \quad k = 1, \ldots, N_l - 1. \quad (14)$$

These models will be denoted as $LM1 - LM4$, where M means mixed models based on Reissner's mixed variational theorem.

ESL Mixed Theories

Mixed theories with ESL description can be used by referring to the displacement model at Equation (5) and layer-wise stress assumptions at Equation (13). These will be referred to as $EMC1 - EMC4$. In case of displacement model with ZZ shape as Equation (8), the relative theories will be indicated as $EMZC1 - EMZC3$. In this case the letter C is added to remark the continuity of transverse shear/normal stresses.

RESULTS AND DISCUSSION

The above models have been coded according to CUF. Details can be found in previous authors' works [32–36] and [14].

In this section two different shell geometries will be considered: a curved shell panel denoted as Ren shell and a cylindrical shell well-known as Varadan–Baskar shell. These two problems were originally considered in [39,40], respectively, for the case of cross-ply laminated shells. Figure 1 quotes the geometry and notations for the two considered shells, details on the geometrical data are reported in Table 1. The proposed shells are simply supported with an applied bisinusoidal load in order to obtain closed form solutions.

To make evident the effect of 'soft' core stiffness on the considered kinematics, sandwich shells with various mechanical properties have been analyzed. Results are herein given for the following lay-outs which coincide to the benchmarks selected in this work. The considered benchmarks are about three different FCSR, both cases of Ren shell and Varadan–Baskar cylindrical shell will be considered:

- Benchmark 1 (B1): a core in nomex and two external skins in aluminium alloy Al2024, the material properties are reported in Table 2.
- Benchmark 2 (B2): a reduced stiffness core, obtained dividing the Nomex properties by 100 and the external skins are the same of benchmark 1, the material properties are reported in Table 3.
- Benchmark 3 (B3): three isotropic layers with face-to-core-stiffness-ratio $E_{\text{skin}}/E_{\text{core}} = 50$, the full material data are indicated in Table 4.

A large numerical investigation has been performed to analyze both the effects of shell geometries and mechanical properties on various shell theories kinematics. The most

Table 1. Geometrical data for the two considered shells.

Properties	Ren shell
a (m)	1
$b=\frac{\pi}{3}R_\beta$ (m)	10.47197
R_α (m)	∞
R_β (m)	10
$m(-)$	0
$n(-)$	1
p_z(top)(Pa)	1
	Varadan–Baskar shell
a (m)	40
$b=2\pi R_\beta$ (m)	62.831853
R_α (m)	∞
R_β (m)	10
$m(-)$	1
$n(-)$	8
p_z(top)(Pa)	1(benchmarks)
p_z(bottom)(Pa)	1(assessment)

Table 2. Benchmark 1. Elastic properties of sandwich shell with core in Nomex. $\frac{E_{\text{skin}}}{E_{T\text{core}}}=73E^5$.

Properties	Layer 1–3 (Al 2024)
E (GPa)	73
ν	0.34
G (GPa)	27.239
$\frac{h_1}{h_{tot}}=\frac{h_3}{h_{tot}}$ $(-)$	0.1
	Layer 2 (Nomex)
$E_L=E_T$ (MPa)	0.01
E_z (MPa)	75.85
ν	0.01
G (MPa)	22.5
$\frac{h_2}{h_{tot}}$ $(-)$	0.8

Table 3. Benchmark 2. Elastic properties of sandwich shell with reduced stiffness core. $\frac{E_{\text{skin}}}{E_{T\text{core}}}=73E^7$.

Properties	Layer 1–3 (Al 2024)
E (GPa)	73
ν	0.34
G (GPa)	27.239
$\frac{h_1}{h_{tot}}=\frac{h_3}{h_{tot}}$ $(-)$	0.1
	Layer 2 (core divided by 100)
$E_L=E_T$ (MPa)	0.0001
E_z (MPa)	0.7585
ν	0.01
G (MPa)	0.225
$\frac{h_2}{h_{tot}}$ $(-)$	0.8

Table 4. Benchmark 3. Elastic properties of isotropic sandwich shell. $\frac{E_{skin}}{E_{Tcore}} = 50$.

Properties	Layer 1–3
E (GPa)	50
ν	0.25
G (GPa)	20
$\frac{h_1}{h_{tot}} = \frac{h_3}{h_{tot}}$ (–)	0.1
	Layer 2
E (GPa)	1
ν	0.25
G (MPa)	0.4
$\frac{h_2}{h_{tot}}$ (–)	0.8

significant results are discussed in the following. These have been, for convenience, grouped in three main subsections, which are devoted to discuss, global deflections, stresses, through-the-thickness distributions of stress, and displacement components, respectively.

Evaluation of Maximum Transverse Deflections

The CUF considered in this work has been applied to laminated shells in [41,42]. The last work also provides assessments with available 3D exact solutions. However, no 3D solution is available for the benchmarks considered in this work. A layer-wise mixed theory with fourth-order of expansion for both displacement and transverse stress variables ($LM4$) will therefore used as quasi 3D solution in the subsequent analyses. To show the effectiveness of $LM4$ results for the laminated cross-ply shell, the case of paper [40] is reconsidered. The geometrical data are those in Table 1 and the material properties are given in Table 5; it is a three-layered cylindrical shell (fiber orientation $90°/0°/90°$) with a bi-sinusoidal transverse distribution of pressure loadings applied at its bottom surface. Table 6 quotes the transverse displacement at middle-surface (the 3D solution is by Varadan-Baskar [40]). It is clearly shown that the $LM4$ model gives a 3D evaluation for the static response of a multilayered shell. This result permits us to refer to $LM4$ solutions as a 3D one in the three benchmarks considered in this article.

Maximum shell transverse deflection, or amplitude, for the various benchmarks and various geometrical parameters are discussed below.

CLASSICAL THEORIES

The CLT and the FSDT are investigated in Tables 7–9 and in Tables 10–12 for the Ren case and the Varadan–Baskar one, respectively. So called thickness locking or Poisson locking phenomena has been removed according to what in [35,36].

Both shells have been investigated to foresee the possible differences between curved panels and cylindrical shells. In Tables 7–12 is clearly shown the inadequacy of classical theories in case of low values of LTR, and the importance of the FCSR parameter even if the shell is very thin: error of 11.5% is found in the B2 sandwich for R_β/h=1000. For the same geometries errors of 0.03% and 0.33% are found for the B1 and B3 sandwiches, respectively. Improvements, but not very significant, of FSDT analyses are registred in the

Table 5. Assessment. Elastic properties of the three layered shell with fiber orientation 90°/0°/90°.

Properties	Layer 1-2-3
E_L (GPa)	172
E_T (GPa)	6.9
G_{LT} (GPa)	3.4
G_{TT} (GPa)	1.4
ν_{LT} (−)	0.25
ν_{TT} (−)	0.25
$\frac{h_1}{h_{tot}} = \frac{h_2}{h_{tot}} = \frac{h_3}{h_{tot}}$ (−)	$\frac{1}{3}$

Table 6. Assessment. Varadan and Baskar shell with mechanical load applied at the bottom.

R_β/h	2	Error (%)	4	Error (%)	10	Error (%)	50	Error (%)	100	Error (%)
					$\overline{U}_z = U_z(10E_L h^3/P_{zb}R_\beta^4)$ at $z=0$					
3D [40]	10.110	–	4.0090	–	1.2230	–	0.5395	–	0.4715	–
*LM*3	10.080	(0.30)	4.0082	(0.02)	1.2233	(0.02)	0.5395	(0.00)	0.4715	(0.00)
*LM*4	10.106	(0.04)	4.0089	(0.00)	1.2232	(0.01)	0.5395	(0.00)	0.4715	(0.00)

Table 7. Benchmark 1. Ren shell with $\frac{E_{skin}}{E_{Tcore}} = 73E^5$. 3D vs. classical theories.

R_β/h	4	Error (%)	10	Error (%)	50	Error (%)	100	Error (%)	1000	Error (%)
					$\overline{U}_z = U_z(10E_{skin}h^3/P_{zt}R_\beta^4)$ at $z=0$					
3D	234.88	–	47.587	–	5.2040	–	3.8562	–	3.4008	–
CLT	3.7775	(98.4)	3.5612	(92.5)	3.4318	(34.0)	3.4150	(11.4)	3.3998	(0.03)
FSDT	5.0668	(97.8)	3.7577	(92.1)	3.4393	(33.9)	3.4168	(11.3)	3.3998	(0.03)

Table 8. Benchmark 2. Ren shell with $\frac{E_{skin}}{E_{Tcore}} = 73E^7$. 3D vs. classical theories.

R_β/h	4	Error (%)	10	Error (%)	50	Error (%)	100	Error (%)	1000	Error (%)
					$\overline{U}_z = U_z(10E_{skin}h^3/P_{zt}R_\beta^4)$ at $z=0$					
3D	447.95	–	730.82	–	149.89	–	45.342	–	3.8412	–
CLT	3.7775	(99.2)	3.5612	(99.5)	3.4318	(97.7)	3.4149	(92.5)	3.3998	(11.5)
FSDT	5.0709	(98.9)	3.7583	(99.4)	3.4393	(97.7)	3.4168	(92.4)	3.3998	(11.5)

Table 9. Benchmark 3. Ren shell with $\frac{E_{skin}}{E_{core}} = 50$. 3D vs. classical theories.

R_β/h	4	Error (%)	10	Error (%)	50	Error (%)	100	Error (%)	1000	Error (%)
					$\overline{U}_z = U_z(10E_{skin}h^3/P_{zt}R_\beta^4)$ at $z=0$					
3D	15.770	–	5.5450	–	3.6352	–	3.5635	–	3.5180	–
CLT	3.9200	(75.1)	3.6971	(33.3)	3.5630	(1.99)	3.5456	(0.50)	3.5297	(0.33)
FSDT	5.0400	(68.0)	3.8675	(30.2)	3.5696	(1.80)	3.5472	(0.46)	3.5298	(0.33)

Table 10. Benchmark 1. Varadan and Baskar shell with $\frac{E_{skin}}{E_{Tcore}} = 73E^5$. 3D vs. classical theories.

R_β/h	4	Error (%)	10	Error (%)	50	Error (%)	100	Error (%)	1000	Error (%)
					$\overline{U}_z = U_z(10E_{skin}h^3/P_{zt}R_\beta^4)$ at $z=0$					
3D	90.170	–	20.465	–	1.5798	–	0.8539	–	0.0349	–
CLT	0.9947	(98.9)	0.9351	(95.4)	0.8507	(46.1)	0.7210	(15.6)	0.0349	(0.00)
FSDT	1.6215	(98.2)	1.0300	(95.0)	0.8540	(45.9)	0.7216	(15.5)	0.0349	(0.00)

Table 11. Benchmark 2. Varadan and Baskar shell with $\frac{E_{skin}}{E_{Tcore}} = 73E^7$. 3D vs. classical theories.

R_β/h	4	Error (%)	10	Error (%)	50	Error (%)	100	Error (%)	1000	Error (%)
					$\overline{U}_z = U_z(10E_{skin}h^3/P_{zt}R_\beta^4)$ at $z=0$					
3D	378.99	–	134.26	–	11.912	–	3.0995	–	0.0352	–
CLT	0.9948	(99.7)	0.9351	(99.3)	0.8508	(92.9)	0.7210	(76.7)	0.0349	(0.85)
FSDT	1.6234	(99.6)	1.0304	(99.2)	0.8540	(92.8)	0.7216	(76.7)	0.0349	(0.85)

Table 12. Benchmark 3. Varadan and Baskar shell with $\frac{E_{skin}}{E_{core}} = 50$. 3D vs. classical theories.

R_β/h	4	Error (%)	10	Error (%)	50	Error (%)	100	Error (%)	1000	Error (%)
					$\overline{U}_z = U_z(10E_{skin}h^3/P_{zt}R_\beta^4)$ at $z=0$					
3D	6.5880	–	1.8460	–	0.9097	–	0.7389	–	0.0327	–
CLT	1.0339	(84.3)	0.9719	(47.3)	0.8787	(3.41)	0.7330	(0.80)	0.0327	(0.00)
FSDT	1.5784	(76.0)	1.0543	(42.9)	0.8815	(3.10)	0.7335	(0.73)	0.0327	(0.00)

thick shell cases. Differences between curved panels and cylindrical shells cases barely appear, therefore only Ren type panels are analyzed in the following.

HIGHER ORDER THEORIES

HOT are investigated in Tables 13 and 14 for the B1 and B2 sandwiches, respectively. Linear up-to forth order of expansions are considered. Theories that include Murakami's zig-zag functions are investigated too. The effect of neglecting thickness strains ϵ_{zz} has been evaluated in same cases; related theories are depicted by suffix *d*. The following comments can be made. The error remains very high in case of *ED*1–*ED*4 theories. Significant improvements are introduced by the use of MZZF, that permits to introduce the ZZ effects for a sandwich structure. In case of high FCSR values the error remains high, however in the *EDZ*3 model the error is <2% in case of thin shell.

LAYER WISE THEORIES

The results in Tables 15 and 16 clearly show that the use of layer wise models is mandatory in the case of sandwich shells. The accuracy of layer-wise analysis is, in fact, independent by the FCSR values: excellent agreement with 3D solution has been found in both B1 and B2 cases. Layer Wise models permit, in fact, to see separately each layer; as a consequence ZZ effect is intrinsically considered by these models.

Table 13. Benchmark 1. Ren shell with $\frac{E_{skin}}{E_{Tcore}} = 73E^5$. 3D vs. ESL models.

R_β/h	10	Error (%)	100	Error (%)
		$\overline{U}_z = U_z(10E_{skin}h^3/P_{zt}R_\beta^4)$ at $z=0$		
3D	47.587	–	3.8562	–
*ED*1	3.7621	(92.1)	3.4169	(11.4)
*ED*4	8.5193	(82.1)	3.4650	(10.1)
*EDZ*1	27.321	(42.6)	3.8548	(0.04)
*EDZ*3	46.761	(1.74)	3.8577	(0.04)
*ED*1*d*	3.7577	(92.1)	3.4168	(11.4)
*EDZ*1*d*	34.065	(28.4)	3.8617	(0.14)

Table 14. Benchmark 2. Ren shell with $\frac{E_{skin}}{E_{Tcore}} = 73E^7$. 3D vs. ESL models.

R_β/h	10	Error (%)	100	Error (%)
		$\overline{U}_z = U_z(10E_{skin}h^3/P_{zt}R_\beta^4)$ at z = 0		
3D	730.82	–	45.342	–
ED1	3.7627	(99.5)	3.4169	(92.5)
ED4	9.0849	(98.8)	3.4688	(92.3)
EDZ1	858.02	(17.4)	27.338	(39.7)
EDZ3	537.00	(26.5)	44.538	(1.77)
ED2d	3.7587	(99.5)	3.4169	(92.5)
EDZ2d	703.04	(3.80)	45.944	(1.33)

Table 15. Benchmark 1. Ren shell with $\frac{E_{skin}}{E_{Tcore}} = 73E^5$. 3D vs. LW models.

R_β/h	4	Error (%)	100	Error (%)
		$\overline{U}_z = U_z(10E_{skin}h^3/P_{zt}R_\beta^4)$ at $z=0$		
3D	234.88	–	3.8562	–
*LD*1	213.16	(8.95)	3.8498	(0.16)
*LD*2	234.87	(0.00)	3.8562	(0.00)
*LD*3	234.89	(0.00)	3.8562	(0.00)
*LD*4	234.88	(0.00)	3.8562	(0.00)

Table 16. Benchmark 2. Ren shell with $\frac{E_{skin}}{E_{Tcore}} = 73E^7$. 3D vs. LW models.

R_β/h	4	Error (%)	100	Error (%)
		$\overline{U}_z = U_z(10E_{skin}h^3/P_{zt}R_\beta^4)$ at z = 0		
3D	447.95	–	45.342	–
LD1	104.76	(76.6)	44.468	(1.93)
LD2	447.53	(0.09)	45.342	(0.00)
LD3	447.89	(0.01)	45.342	(0.00)
LD4	447.95	(0.00)	45.342	(0.00)

MIXED THEORIES

The mixed theories based on RMVT are considered in Tables 17–20. Both ESL and LW results are given. Improvement are obtained with respect to PVD theories. However, ESL

Table 17. Benchmark 1. Ren shell with $\frac{E_{skin}}{E_{Tcore}} = 73E^5$. 3D vs. Mixed ESL models.

R_β/h	10	Error (%)	100	Error (%)
		$\overline{U}_z = U_z(10E_{skin}h^3/P_{zt}R_\beta^4)$ at $z=0$		
3D	47.587	–	3.8562	–
*EMC*1	4.0999	(91.4)	3.6789	(4.60)
*EMC*4	9.2064	(80.6)	3.4718	(9.97)
*EMZC*1	30.141	(36.7)	3.9627	(2.76)
*EMZC*3	46.873	(1.50)	3.8577	(0.04)

Table 18. Benchmark 2. Ren shell with $\frac{E_{skin}}{E_{Tcore}} = 73E^7$. 3D vs. Mixed ESL models.

R_β/h	10	Error (%)	100	Error (%)
		$\overline{U}_z = U_z(10E_{skin}h^3/P_{zt}R_\beta^4)$ at $z=0$		
3D	730.82	–	45.342	–
*EMC*1	4.1010	(99.4)	3.6788	(91.9)
*EMC*4	9.9477	(98.6)	3.4773	(92.3)
*EMZC*1	972.33	(33.0)	29.830	(34.2)
*EMZC*3	557.33	(23.7)	44.644	(1.54)

Table 19. Benchmark 1. Ren shell with $\frac{E_{skin}}{E_{Tcore}} = 73E^5$. 3D vs. Mixed LW models.

R_β/h	4	Error (%)	100	Error (%)
		$\overline{U}_z = U_z(10E_{skin}h^3/P_{zt}R_\beta^4)$ at $z=0$		
3D	234.88	–	3.8562	–
*LM*1	233.41	(0.62)	3.8562	(0.00)
*LM*2	234.88	(0.00)	3.8562	(0.00)
*LM*3	234.88	(0.00)	3.8562	(0.00)
*LM*4	234.88	(0.00)	3.8562	(0.00)

Table 20. Benchmark 2. Ren shell with $\frac{E_{skin}}{E_{Tcore}} = 73E^7$. 3D vs. Mixed LW models.

R_β/h	4	Error (%)	100	Error (%)
		$\overline{U}_z = U_z(10E_{skin}h^3/P_{zt}R_\beta^4)$ at $z=0$		
3D	447.95	–	45.342	–
*LM*1	530.79	(18.5)	45.342	(0.00)
*LM*2	447.93	(0.00)	45.342	(0.00)
*LM*3	447.89	(0.00)	45.342	(0.00)
*LM*4	447.95	(0.00)	45.342	(0.00)

Table 21. Benchmark 1. Ren shell with $\frac{E_{skin}}{E_{Tcore}} = 73E^5$. 3D vs. Mixed ESL models.

R_β/h	10	Error (%)	100	Error (%)
		$\overline{\sigma}_{\beta z} = \sigma_{\beta z}(h/P_{zt}R_\beta)$ at $z=0$		
3D	0.4125	–	0.4168	–
*EMC*1	0.0023	(99.4)	0.0022	(99.5)
*EMC*4	0.0679	(83.5)	0.0654	(84.3)
*EMCZ*1	0.2187	(47.0)	0.4136	(0.77)
*EMCZ*3	0.4069	(1.36)	0.4169	(0.00)

Table 22. Benchmark 2. Ren shell with $\frac{E_{skin}}{E_{Tcore}} = 73E^7$. 3D vs. Mixed ESL models.

R_β/h	10	Error (%)	100	Error (%)
		$\overline{\sigma}_{\beta z} = \sigma_{\beta z}(h/P_{zt}R_\beta)$ at $z=0$		
3D	0.0655	–	0.3960	–
*EMC*1	2.3E-5	(99.9)	2.2E-5	(99.9)
*EMC*4	7.7E-4	(98.8)	7.5E-4	(99.8)
*EMCZ*1	0.1019	(55.6)	0.2236	(43.5)
*EMCZ*3	0.0464	(29.2)	0.3892	(1.72)

Table 23. Benchmark 1. Ren shell with $\frac{E_{skin}}{E_{Tcore}} = 73E^5$. 3D vs. Mixed LW models.

R_β/h	10	Error (%)	100	Error (%)
		$\overline{\sigma}_{\beta z} = \sigma_{\beta z}(h/P_{zt}R_\beta)$ at $z=0$		
3D	0.4125	–	0.4168	–
*LM*1	0.4131	(0.14)	0.4168	(0.00)
*LM*2	0.4130	(0.12)	0.4168	(0.00)
*LM*3	0.4125	(0.00)	0.4168	(0.00)
*LM*4	0.4125	(0.00)	0.4168	(0.00)

Table 24. Benchmark 2. Ren shell with $\frac{E_{skin}}{E_{Tcore}} = 73E^7$. 3D vs. Mixed LW models.

R_β/h	10	Error (%)	100	Error (%)
		$\overline{\sigma}_{\beta z} = \sigma_{\beta z}(h/P_{zt}R_\beta)$ at $z=0$		
3D	0.0655	–	0.3960	–
*LM*1	0.0655	(0.00)	0.3960	(0.00)
*LM*2	0.0655	(0.00)	0.3960	(0.00)
*LM*3	0.0655	(0.00)	0.3960	(0.00)
*LM*4	0.0655	(0.00)	0.3960	(0.00)

Table 25. Benchmark 1. Ren shell with $\frac{E_{skin}}{E_{Tcore}} = 73E^5$. 3D vs. Mixed LW models.

R_β/h	10	Error (%)	100	Error (%)
		σ_{zz} at $z = h/2$		
3D	1.0000	–	1.0000	–
*LM*1	0.8394	(16.1)	0.8258	(17.4)
*LM*2	1.0342	(3.42)	1.0043	(0.43)
*LM*3	1.0008	(0.08)	1.0000	(0.00)
*LM*4	1.0000	(0.00)	1.0000	(0.00)

Table 26. Benchmark 2. Ren shell with $\frac{E_{skin}}{E_{Tcore}} = 73E^7$. 3D vs. Mixed LW models.

R_β/h	10	Error (%)	100	Error (%)
		σ_{zz} at $z = h/2$		
3D	1.0000	–	1.0000	–
*LM*1	−8.5890	(>100)	−5.2561	(>100)
*LM*2	1.1314	(13.14)	1.0120	(1.20)
*LM*3	0.9993	(0.07)	1.0000	(0.00)
*LM*4	1.0000	(0.00)	1.0000	(0.00)

analyses remains still poor with improvements in those cases in which MZZF is not used. To notice that LM4 results coincide with 3D ones as definition.

Transverse Stress Evaluations

Mixed models permit '*a priori*' evaluation of transverse stresses, both shear and normal components. Related results are illustrated in Tables 21–26. Benchmark 1 and 2 have been investigated. It is shown that among the various theories considered in this work, the layer-wise theories are the only one able to describe transverse stresses in soft core sandwich shells.

Through-the-thickness Distribution

A summary of the comparisons of various theories to evaluate the through the thickness distribution (core and faces) of displacement and stress components is given in Figures 2–7. Thick and thin shell results are compared. Figures 2 and 3 show the evaluation of transverse displacement along the thickness direction. Significant theories are compared. It is confirmed that a 3D response is only possible with the use of LWMs. The improvements of the MZZF are very much evident, in particular for thin shell and B1 cases. Transverse shear stresses are evaluated in Figures 4 and 5. It is shown that the differences among the various theories are very much influenced by the value of the z-coordinate. Only mixed theories are compared. The same is done in Figures 6–7 in the case of transverse normal stress, layerwise mixed models give a 3D response for both benchmarks 1 and 2.

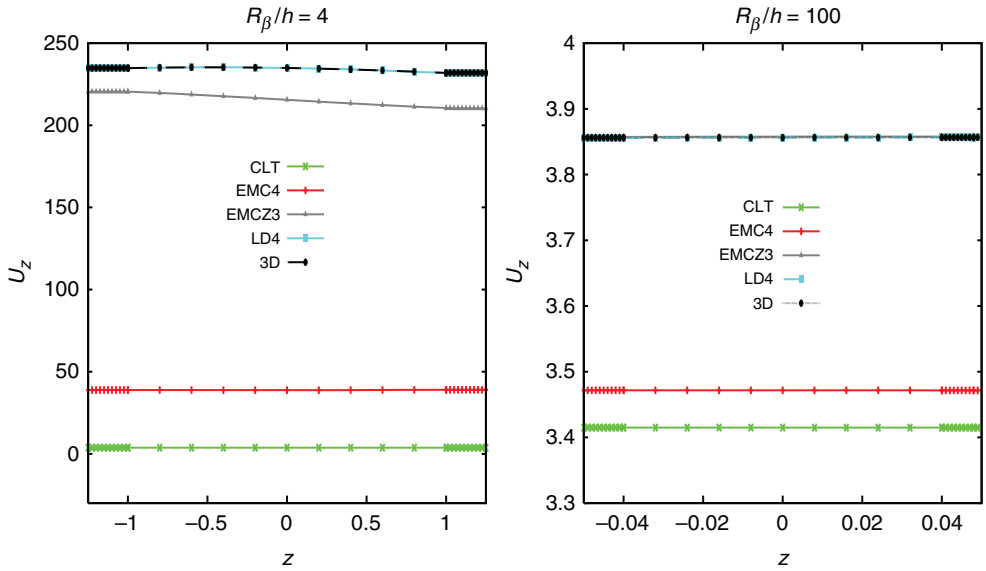

Figure 2. *Benchmark 1. Ren shell with* $\frac{E_{skin}}{E_{Tcore}} = 73E^5$. $\overline{U}_z = U_z(10E_{skin}h^3/P_{zt}R_\beta^4)$ *vs z.*

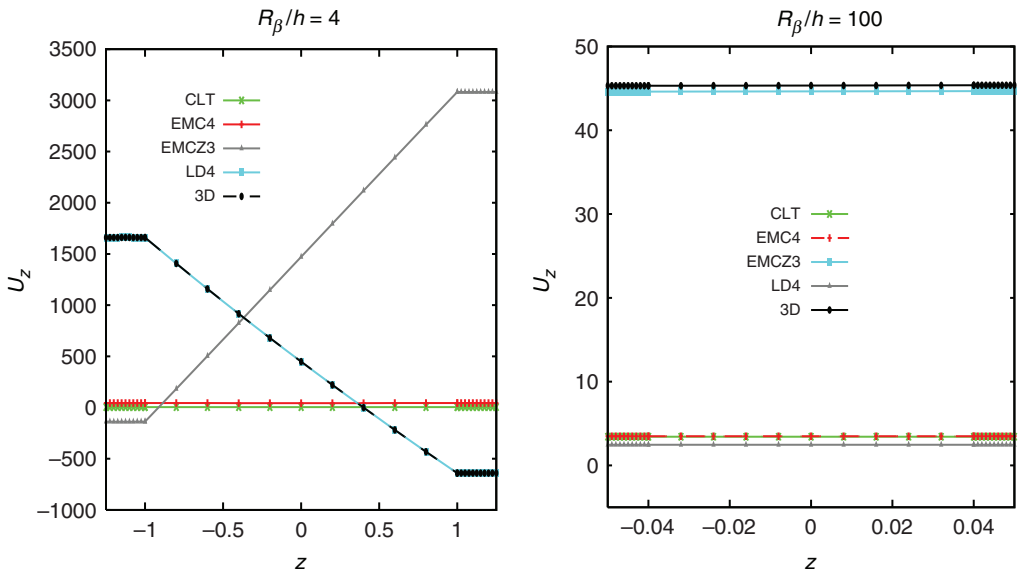

Figure 3. *Benchmark 2. Ren shell with* $\frac{E_{skin}}{E_{Tcore}} = 73E^7$. $\overline{U}_z = U_z(10E_{skin}h^3/P_{zt}R_\beta^4)$ *vs z.*

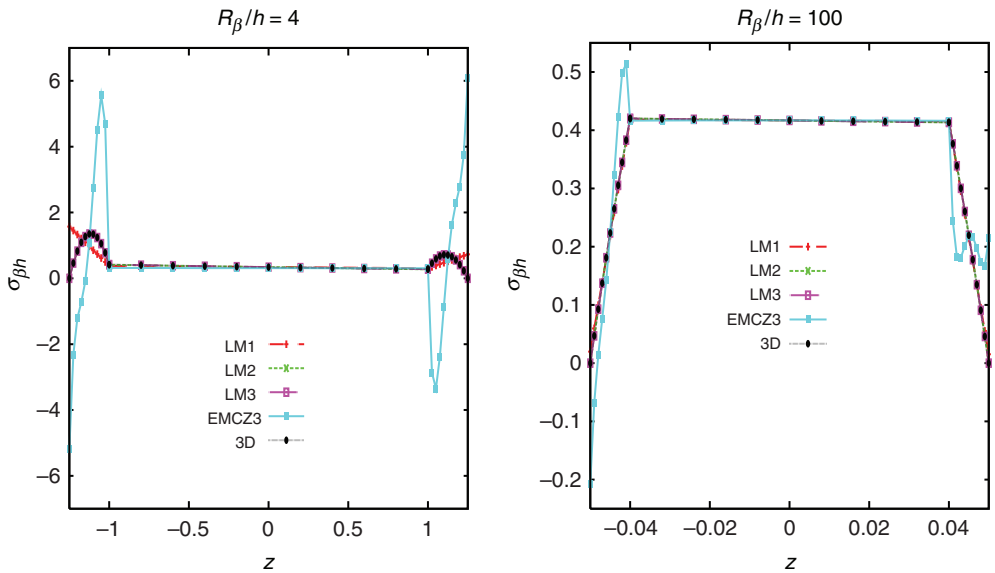

Figure 4. *Benchmark 1. Ren shell with* $\frac{E_{skin}}{E_{Tcore}} = 73E^5$. $\overline{\sigma}_{\beta z} = \sigma_{\beta z}(h/P_{zt}R_\beta)$ *vs z.*

CONCLUSIONS

A numerical assessment of classical, higher-order, ZZ, layer-wise and mixed theories has been considered in this article for the bending of multilayered sandwich curved panels. Several benchmarks, related to different values of the mechanical properties between the face and core (FCSR) and the geometrical ones (LTR), have been analyzed. The following main conclusions can be drawn.

(1) It appears clear that there are two sources of error in the 2D modeling of sandwich shells: the first is related to the LTR, and the second is related to the stiffness ratio between the core and skins (FCSR).
(2) The numerical investigation has shown that the first error can be contrasted by the use of higher order models, while the second source of error can only be contrasted by the use of layer-wise kinematics.
(3) The use of MZZF appears extremely convenient in some cases.
(4) CLT and FSDT cannot be effectively used for the analysis of sandwich structures.

ACKNOWLEDGMENTS

This work has been carried out in the framework of STREP EU project CASSEM under contract NMP-CT-2005-013517, and two regional projects Piemonte 2004: E40 and E59. The help of Salvatore Vitale to carry out some of the made numerical analyses is also acknowledged.

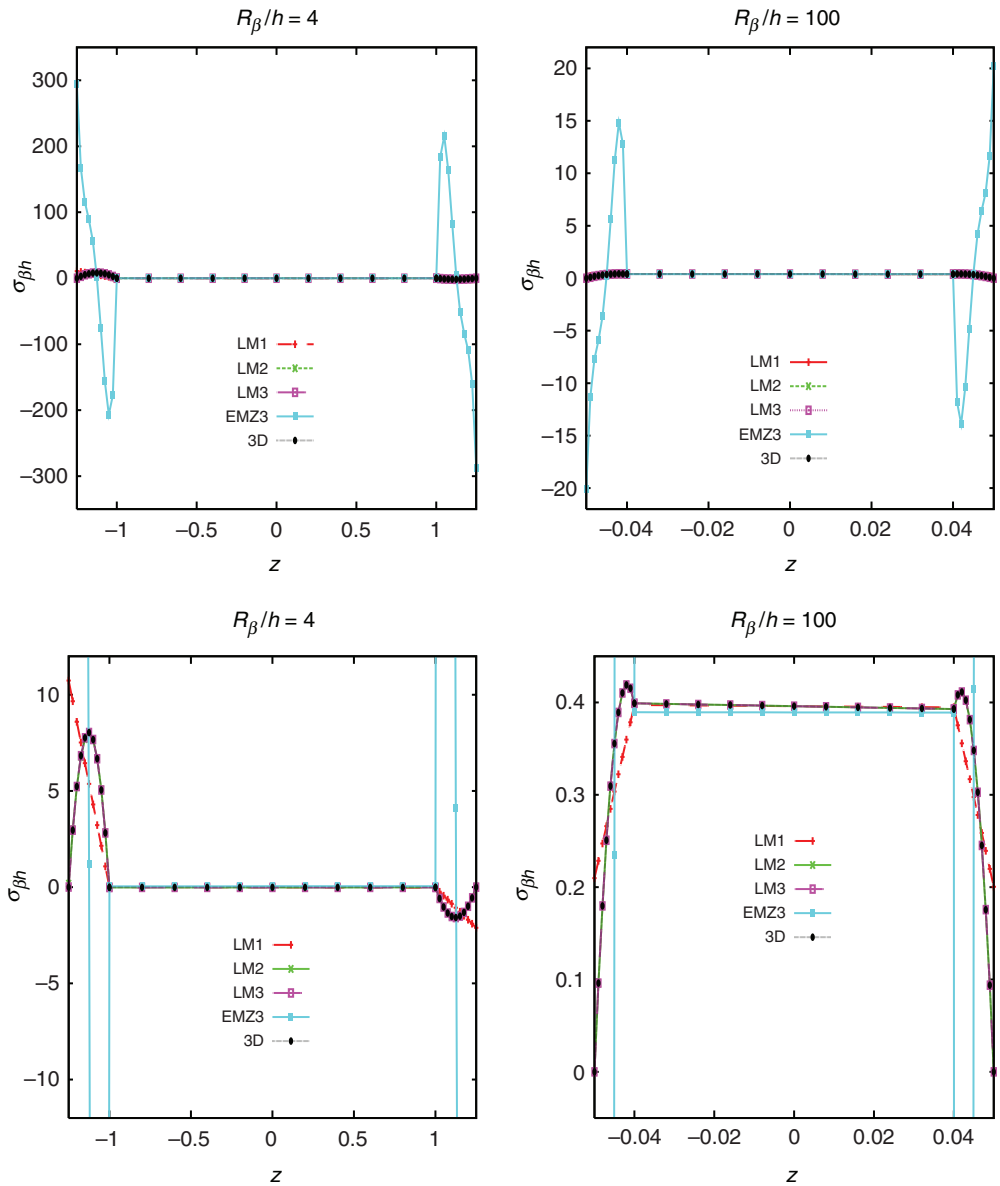

Figure 5. *Benchmark 2. Ren shell with* $\frac{E_{skin}}{E_{Tcore}} = 73E^7$. $\overline{\sigma}_{\beta z} = \sigma_{\beta z}(h/P_{zt}R_\beta)$ *vs z. The two bottom figures zoom the two top ones, respectively.*

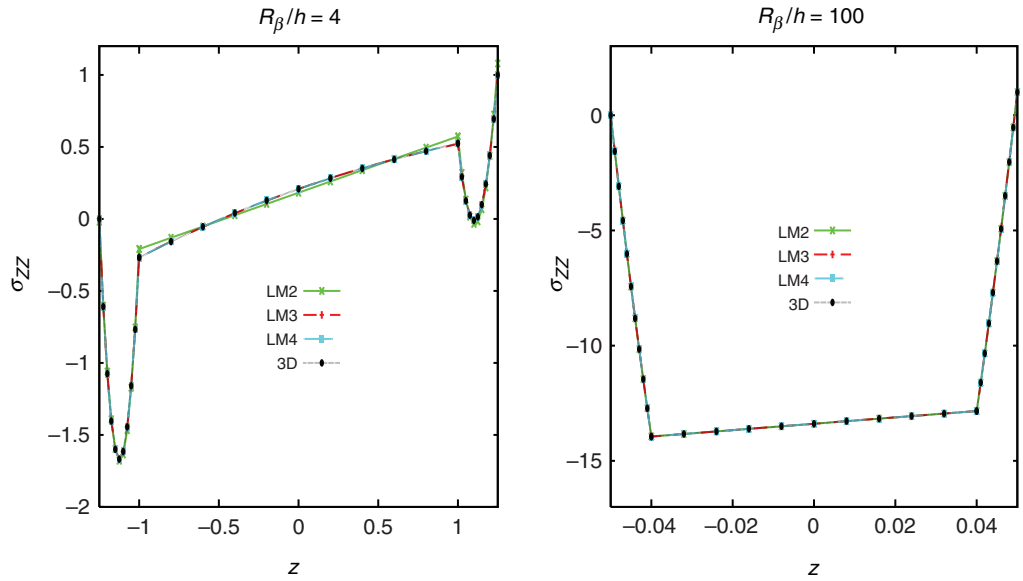

Figure 6. *Benchmark 1. Ren shell with* $\frac{E_{skin}}{E_{Tcore}} = 73E^5$. σ_{zz} *vs z.*

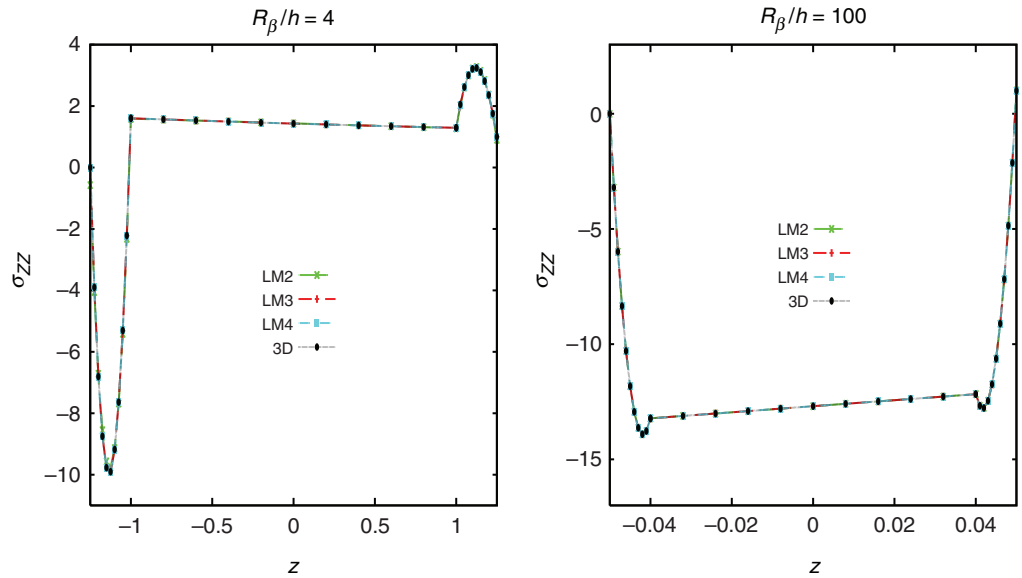

Figure 7. *Benchmark 2. Ren shell with* $\frac{E_{skin}}{E_{Tcore}} = 73E^7$. σ_{zz} *vs z.*

REFERENCES

1. Plantema, F.J. (1966). *Sandwich Construction*, John Wiley & Sons, Inc., New York, USA.
2. Allen, H.G. (1969). *Analysis and Design of Structural Sandwich Panels*, Pergamon Press, London, UK.
3. Zenkert, D. (1995). *An Introduction to Sandwich Structures*, Chamelon Press, London, UK.
4. Vinson, J.R. (1999). *The behaviour of Sandwich Structures of Isotropic and Composite Materials*, Technomic Publishing Company, Inc., Lancaster, USA.
5. Pagano, N.J. (1970). Exact Solutions for Rectangular Bidirectional Composites and Sandwich Plates, *Journal of Composite Material*, **0**(0): 20–34.
6. Dundrova, V. (1966). Stress and Strain Analysis of Simply Supported Non-homogenous Rectangular Plates on the Basis of Lamé Equations, Theory of Plates and Shells, In: V. Slovenskej, (ed.), *Selected Papers for a Conference in October 1963 in Smolinice*, akademie vied, Bratislava.
7. Meyer-Piening, H.-R. (2004). Application of the Elasticity Solution to Linear Sandwich Beams, Plates and Shells Analysis, *Journal of Sandwich Structures and Materials*, **6**(4): 295–312.
8. Cauchy, A.L. (1828). Sur l'équilibre et le mouvement d'une plaque solide, *Exercises de Mathématique*, **3**: 381–412.
9. Poisson, S.D. (1829). Memoire sur l'équilibre et le mouvement des corps élastique, *Mémoires de l'Académie des Sciences des Paris*, **8**: 357–570.
10. Kirchhoff, G. (1850). Über das Gleichgewicht und die Bewegung einer elastishen Scheibe, *Crelles Journal*, **40**: 51–88.
11. Love, A.E.H. (1927). *The Mathematical Theory of Elasticity*, **4th edn**, Cambridge University Press, Cambridge, UK.
12. Reissner, E. (1945). The Effect of Transverse Shear Deformation on the Bending of Elastic Plates, *Journal of Applied Mechanics*, **12**: 69–76.
13. Mindlin, R.D. (1951). Influence of Rotatory Inertia and Shear in Flexural Motions of Isotropic Elastic Plates, *Journal of Applied Mechanics*, **18**: 31–38.
14. Carrera, E. (1995). A Class of Two-dimensional Theories for Anisotropic Multilayered Plates Analysis, Atti Accademia delle Scienze di Torino, Memorie Scienze Fisiche, **19-20**: 49–87.
15. Lekhnitskii, S.G. (1968). *Anisotropic Plates*, Gordon and Breach Science Publishers, New York, USA.
16. Ambartsumian, S.A. (1961). *Theory of Anisotropic Shells*, Translated from Russian, NASA TTF–118, Fizmatzig, Moskwa.
17. Ambartsumian, S.A. (1969). In: Cheron, T. and Ashton, J.E. (eds), *Theory of Anisotropic Plates*, Technomic Publishing Company, Translated from Russian, Moskwa.
18. Ambartsumian, S.A. (1991). *Fragments of the Theory of Anisotropic Shells*, World Scientific Publishing Co., Singapore.
19. Librescu, L. (1975). *Elasto-statics and Kinetics of Anisotropic and Heterogeneous Shell-type Structures*, Noordhoff International, Leyden, Netherland.
20. Reddy, J.N. (1997). Mechanics of Laminated Composite Plates, *Theory and Analysis*, CRC Press, New York, USA.
21. Carrera, E. (2003). A Historical Review of Zig-zag Theories for Multilayered Plates and Shells, *Applied Mechanics Reviews*, **56**(3): 287–308.
22. Carrera, E. and Brischetto, S. (2009). A Survey with Numerical Assessment of Classical and Refined Theories for the Analysis of Sandwich Plates, *Applied Mechanics Reviews*, **62**(1): 1–17.
23. Zhong, C. and Reimerdes, H.-G. (2007). Stability Behavior of Cylindrical and Conical Sandwich Shells with Flexible Core, *Journal of Sandwich Structures and Materials*, **9**(2): 143–166.
24. Demiray, S., Becker, W. and Hohe, J. (2005). *A Triangular Finite Element for Sandwich Plates Accounting for Transverse Core Compressibility*, In: *Proceedings of the 7th International Conference on Sandwich Structures, Sandwich Structures 7: Advancing with Sandwich Structures and Materials*, Aalborg University, Aalborg, Denmark, pp. 301–310.

25. Frostig, Y. (1999). Bending of Curved Sandwich Panels with a Transversely Flexible Core-closed-form High-order Theory, *Journal of Sandwich Structures and Materials*, **1**(1): 4–41.
26. Hohe, J., Librescu, L. and Oh, S.Y. (2006). Dynamic Buckling of Flat and Curved Sandwich Panels with Transversely Compressible Core, *Composite Structures*, **74**(1): 10–24.
27. Hohe, J. and Librescu, L. (2003). A Nonlinear Theory for Doubly Curved Anisotropic Sandwich Shells with Transverse Compressible Core, *International Journal of Solids and Structures*, **40**(5): 1059–1088.
28. Noor, A.K., Burton, S. and Bert, C.W. (1996). Computational Model for Sandwich Panels and Shells, *Applied Mechanics Reviews*, **49**: 155–199.
29. Reddy, J.N. and Robbins, D.H. (1994). Theories and Computational Models for Composite Laminates, *Applied Mechanics Reviews*, **47**: 147–165.
30. Reissner, E. (1984). On a Certain Mixed Variational Theory and a Proposed Application, *International Journal for Numerical Methods in Engineering*, **20**: 1366–1368.
31. Carrera, E. (2001). Developments, Ideas and Evaluations Based Upon the Reissner's Mixed Variational Theorem in the Modeling of Multilayered Plates and Shells, *Applied Mechanics Reviews*, **54**(4): 301–329.
32. Carrera, E. (1998). Layer-wise Mixed Models for Accurate Vibration Analysis of Multilayered Plates, *Journal of Applied Mechanics*, **65**(4): 820–828.
33. Carrera, E. and Demasi, L. (2002). Classical and Advanced Multilayered Plate Elements Based upon PVD and RMVT. Part 1: Derivation of Finite Element Matrices, *International Journal for Numerical Methods in Engineering*, **55**(2): 191–231.
34. Carrera, E. and Demasi, L. (2002). Classical and Advanced Multilayered Plate Elements Based upon PVD and RMVT. Part 2: Numerical Implementation, *International Journal for Numerical Methods in Engineering*, **55**(3): 253–291.
35. Carrera, E. and Brischetto, S. (2008). Analysis of Thickness Locking in Classical, Refined and Mixed Multilayered Plate Theories, *Composite Structures*, **82**(4): 549–562.
36. Carrera, E. and Brischetto, S. (2008). Analysis of Thickness Locking in Classical, Refined and Mixed Theories for Layered Shells, *Composite Structures*, **85**(1): 83–90.
37. Murakami, H. (1986). Laminated Composite Plate Theory with Improved In-plane Responses, *Journal of Applied Mechanics*, **53**: 661–666.
38. Carrera, E. (2004). On the Use of Murakami's Zig-zag Function in the Modeling of Layered Plates and Shells, *Computer & Structures*, **82**(7-8): 541–554.
39. Ren, J.G. (1987). Exact Solutions for Laminated Cylindrical Shells in Cylindrical Bending, *Composite Science and Technology*, **29**(3): 169–187.
40. Varadan, T.K. and Bhaskar, K. (1991). Bending of Laminated Orthotropic Cylindical Shells, *Composite Structures*, **17**(2): 141–156.
41. Carrera, E. (1999). Multilayered Shell Theories Accounting for Layerwise Mixed Description, Part 1: Governing Equations, *AIAA Journal*, **37**(9): 1107–1116.
42. Carrera, E. (1999). Multilayered Shell Theories Accounting for Layerwise Mixed Description, Part 2: Numerical Evaluations, *AIAA Journal*, **37**(9): 1117–1124.